EMBO reports

scientific report

The Tim21 binding domain connects the preprotein translocases of both mitochondrial membranes

Reinhard Albrecht[1,6], Peter Rehling[2], Agnieszka Chacinska[2], Jan Brix[2], Sergio A. Cadamuro[3], Rudolf Volkmer[4], Bernard Guiard[5], Nikolaus Pfanner[2+] & Kornelius Zeth[1,6++]

[1]Max-Planck-Institut für Biochemie, Abteilung Membranbiochemie, Martinsried, Germany, [2]Institut für Biochemie und Molekularbiologie, Zentrum für Biochemie und Molekulare Zellforschung, Universität Freiburg, Freiburg, Germany, [3]Max-Planck-Institut für Biochemie, Laboratory of Bioorganic Chemistry, Martinsried, Germany, [4]Institut für Medizinische Immunologie, Charité—Universitätsmedizin Berlin, Berlin, Germany, [5]Centre de Génétique Moléculaire, CNRS, Gif-sur-Yvette, France, and [6]Max-Planck-Institut für Entwicklungsbiologie, Abteilung Protein Evolution, Tübingen, Germany

Proteins destined for the mitochondrial matrix are imported by the translocase of the outer membrane—the TOM complex—and the presequence translocase of the inner membrane—the TIM23 complex. At present, there is no structural information on components of the presequence translocase. Tim21, a subunit of the presequence translocase consisting of a membrane anchor and a carboxy-terminal domain exposed to the intermembrane space, directly connects the TOM and TIM23 complexes by binding to the intermembrane space domain of the Tom22 receptor. We crystallized the binding domain of Tim21 of *Saccharomyces cerevisiae* and determined its structure at 1.6 Å resolution. The Tim21 structure represents a new α/β-mixed protein fold with two α-helices flanked by an extended eight-stranded β-sheet. We also identified a core sequence of Tom22 that binds to Tim21. Furthermore, negatively charged amino-acid residues of Tom22 are important for binding to Tim21. Here we suggest a mechanism for the TOM–TIM interaction.

Keywords: contact sites; mitochondria; presequence translocase; Tim21; TOM

EMBO reports (2006) **7**, 1233–1238. doi:10.1038/sj.embor.7400828

[1]Max-Planck-Institut für Biochemie, Abteilung Membranbiochemie, Am Klopferspitz 18, D-82512 Martinsried, Germany
[2]Institut für Biochemie und Molekularbiologie, Zentrum für Biochemie und Molekulare Zellforschung, Universität Freiburg, Hermann-Herder-Straße 7, D-79104 Freiburg, Germany
[3]Max-Planck-Institut für Biochemie, Laboratory of Bioorganic Chemistry, Am Klopferspitz 18, D-82512 Martinsried, Germany
[4]Institut für Medizinische Immunologie, Charité—Universitätsmedizin Berlin, Hessische Straße 3–4, D-10115 Berlin, Germany
[5]Centre de Génétique Moléculaire, CNRS, Avenue de la Terrasse—Bât. 26, F-91190 Gif-sur-Yvette, France
[6]Max-Planck-Institut für Entwicklungsbiologie, Abteilung Protein Evolution, Spemannstraße 35/I, D-72076 Tübingen, Germany
[+]Corresponding author. Tel: +49 761 2035224; Fax: +49 761 2035261; E-mail: nikolaus.pfanner@biochemie.uni-freiburg.de
[++]Corresponding author. Tel: +49 7071 601 323; Fax: +49 7071 601 349; E-mail: kornelius.zeth@tuebingen.mpg.de

Received 10 April 2006; revised 11 August 2006; accepted 8 September 2006; published online 10 November 2006

INTRODUCTION

The mitochondria import about 1,000 different precursor proteins from the cytosol, and the translocase of the outer membrane—the TOM complex—functions as the general import gate of the outer membrane. From here, the precursor proteins are distributed to four different translocases and sorting machineries (Neupert, 1997; Jensen & Johnson, 2001; Koehler, 2004; Rehling *et al*, 2004)—(i) the precursors of β-barrel proteins are transferred to the sorting and assembly machinery (SAM complex) that mediates integration into the outer membrane; (ii) small proteins of the intermembrane space (IMS) use the mitochondrial IMS import and assembly machinery; (iii) hydrophobic carrier proteins interact with the Tim9–Tim10 complex of the IMS and are inserted into the inner membrane by the twin-pore translocase; and (iv) the main mitochondrial protein import pathway involves cleavable targeting signals (presequences) at the amino termini of preproteins. The TIM23 complex mediates the translocation of the preproteins into, or across, the inner membrane. The presequence translocase-associated motor complex (PAM) drives the completion of translocation into the matrix, in which the presequences are proteolytically removed.

Presequence-carrying preproteins are transferred from the TOM complex to the TIM23 complex at translocation contact sites. Although their first description by Schleyer and Neupert (1985) raised significant interest, the molecular nature of translocation contact sites has remained unknown. It was shown that a preprotein arrested during transport across both mitochondrial membranes stably connected the TOM and TIM23 complexes (Rassow *et al*, 1989; Dekker *et al*, 1997; Chacinska *et al*, 2003). Tim50, an essential subunit of the TIM23 complex, interacts with preproteins on their emergence on the IMS side of the outer membrane; however, Tim50 does not form a direct contact with the TOM complex (Koehler, 2004; Rehling *et al*, 2004). The identification of Tim21 provided the first evidence for a direct contact between TOM and TIM23 complexes (Chacinska *et al*, 2005).

Tim21 consists of a single transmembrane segment in the inner membrane, and a large IMS domain that has been shown to bind to the IMS domain of the outer membrane of the Tom22 receptor (Chacinska *et al*, 2005; Mokranjac *et al*, 2005). This interaction is required for efficient cell growth under conditions that require high mitochondrial activity (Chacinska *et al*, 2005). Presequence peptides inhibit the Tim21–Tom22 interaction (Chacinska *et al*, 2005), suggesting a regulatory role for Tim21 in protein import. However, the nature and mechanism of the TOM–TIM interaction remain unknown owing to the current lack of detailed structural information of most components of the mitochondrial protein import machinery, which has strongly limited a mechanistic understanding of the import process. So far, only five high-resolution structures have been reported: the cytosolic domains of the receptors Tom20 and Tom70 (Abe *et al*, 2000; Perry *et al*, 2006; Wu & Sha, 2006); the Tim9–Tim10 chaperone complex (Webb *et al*, 2006); the carboxy-terminal domain of Tim44 of the motor PAM (Josyula *et al*, 2006); and the matrix processing peptidase (Taylor *et al*, 2001). Here, we report the structure of the IMS domain of Tim21 at 1.6 Å resolution and propose a mechanism for the TOM–TIM interaction.

RESULTS AND DISCUSSION

Crystallization of the Tim21 binding domain

We expressed the full-length IMS domain of *Saccharomyces cerevisiae* Tim21 (residues 103–239) with an N-terminal His tag. This domain binds to the IMS domain of Tom22 (Chacinska *et al*, 2005). A concentrated solution of the purified Tim21 domain was subjected to various crystallization screens, but no crystals were obtained. As flexible termini often prevent proteins from crystallizing, we used subtilisin to tentatively remove terminal amino-acid residues and obtained a protease-resistant domain. Analysis using mass spectrometry identified two fragments—residues 103–227 and 103–225. The shorter fragment, termed $Tim21_{IMS}$, was expressed with an N-terminal His tag (Fig 1A). We used two assays to analyse whether this domain of Tim21 still contained the TOM interaction site. First, a glutathione *S*-transferase (GST) fusion protein containing $Tom22_{IMS}$ was incubated with $Tim21_{IMS}$ and the mixture was subjected to affinity purification using Ni-NTA chromatography. GST–$Tom22_{IMS}$ was co-eluted with $Tim21_{IMS}$ (Fig 1A). We then analysed the interaction of the untagged domains using ^{1}H NMR spectroscopy. The addition of increasing amounts of $Tim21_{IMS}$ led to significant changes in intensity in several $Tom22_{IMS}$ peaks (Fig 1B), indicating an interaction of both domains. We conclude that $Tim21_{IMS}$ is competent to interact with $Tom22_{IMS}$.

Initial crystallization trials with untagged $Tim21_{IMS}$ did not lead to any crystalline material. However, we noticed that an unusually high number of crystallization drops remained clear, indicating that the protein concentration, although 25–30 mg/ml, was still too low. On concentrating $Tim21_{IMS}$ to approximately 90 mg/ml, cubical-shaped crystals were obtained after 2–4 weeks.

Structure of the Tim21 binding domain

$Tim21_{IMS}$ crystallized in the orthorhombic space group $P2_12_12_1$ with one monomer of the protein in the asymmetric unit (Table 1). We recorded a native data set of the $Tim21_{IMS}$ crystals to a resolution limit of 1.6 Å. The structure was solved by a multi-wavelength anomalous dispersion (MAD) experiment carried out on a seleno-methionine (SeMet)-labelled protein. A large part of the model was built automatically, and subsequent model building enabled us to fit all amino acids of the $Tim21_{IMS}$ chain into the electron density map except for the side chains of three lysine residues (Lys 118, Lys 120 and Lys 193), which could not be localized and were thus modelled as alanine residues. The structure was refined to a crystallographic *R*-factor of 19.7% (R_{free} = 24.8%). The final model consisted of residues 103–225 and

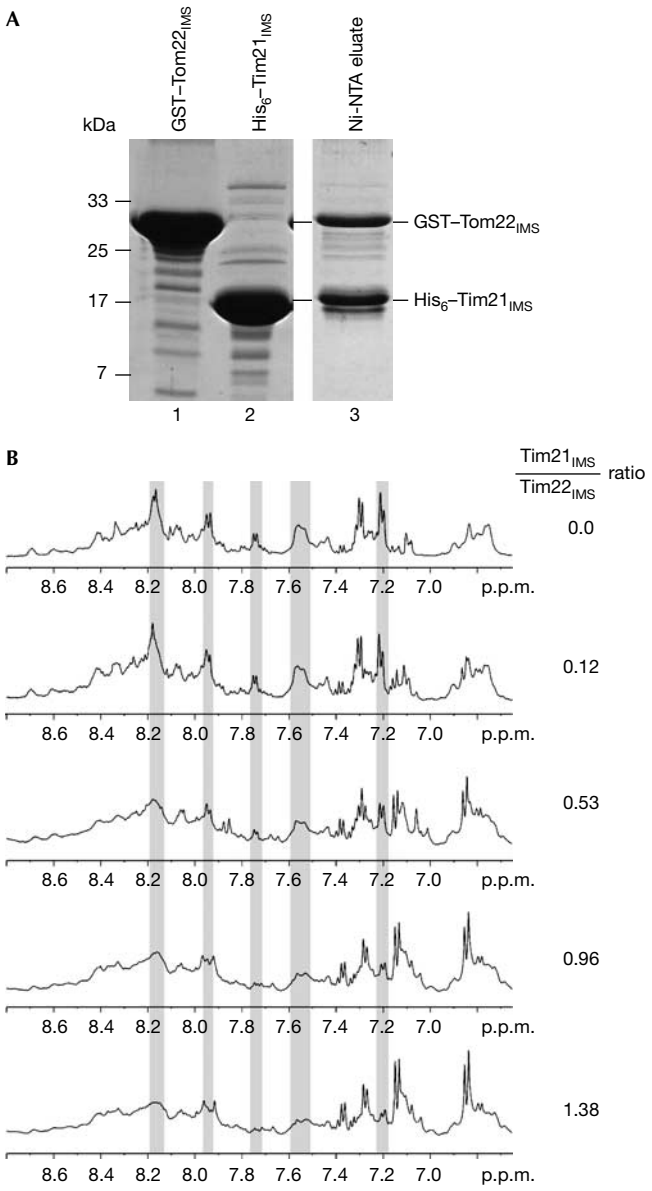

Fig 1 | $Tim21_{IMS}$ interaction with $Tom22_{IMS}$. (**A**) Purified GST–$Tom22_{IMS}$ and His_6–$Tim21_{IMS}$ were mixed and applied to Ni-NTA-agarose. After washing, bound proteins were eluted with imidazole and analysed by SDS–polyacrylamide gel electrophoresis and stained with Coomassie R-250. (**B**) ^{1}H NMR spectroscopic detection of complex formation between $Tim21_{IMS}$ and $Tom22_{IMS}$. Spectra of $Tom22_{IMS}$ were recorded in the absence or presence of $Tim21_{IMS}$. Grey panels indicate changes in peak intensity. GST, glutathione *S*-transferase; $Tim21_{IMS}$, translocase of the inner membrane; $Tom22_{IMS}$, translocase of the outer membrane.

Table 1 | Statistics of data collection and refinement on $Tim21_{IMS}$

Data collection		**SeMet crystal**		**Native crystal**
Space group		$P2_12_12_1$		$P2_12_12_1$
Unit cell constants				
a (Å)		32.1		32.3
b (Å)		59.2		58.8
c (Å)		62.6		62.6
	Inflection	Peak	Remote	
Wavelength (Å)	0.9794	0.9792	0.9763	1.05
Resolution (Å)	1.9	1.9	1.9	1.58
	(2.02–1.9)	(2.02–1.9)	(2.02–1.9)	(1.68–1.58)
Unique reflections	9,503	9,785	9,541	16,515
Completeness (%)	96.2	99.4	96.4	97.5
	(85.7)	(97.2)	(88.3)	(94.0)
Redundancy	3.4	6.8	3.4	3.33
Anomalous diffractors		3		
R_{merge} (%)	4.9 (51)	7.1 (62.3)	5.4 (55.6)	3.8 (26.4)
FOM* (SOLVE)		0.42		
FOM* (RESOLVE)		0.54		
$I/\sigma(I)$	14.48 (2.07)	15.41 (2.42)	13.05 (1.9)	18.0 (3.7)
Refinement statistics				
Resolution range (Å)				20.0–1.6 (1.7–1.6)
No. of reflections used				16,047
No. of reflections in working set				15,244
No. of reflections in test set				803
No. of non-hydrogen protein atoms				1,003
No. of solvent atoms				167
R_{cryst} (%)/R_{free} (%)†				19.7/24.8 (22.2/28.1)
R.m.s.d. of bond lengths (Å)				0.006
R.m.s.d. of bond angles (deg)				1.3
Mean B factor (Å^2)				22.9
Ramachandran plot statistics‡				
Most favoured				111 (91.7%)
Additionally allowed				8 (6.6%)
Generously allowed				2 (1.6%)
Disallowed				0

Values in parentheses refer to the highest resolution shell.
*FOM, figure of merit.
†R_{free} was calculated using 5% randomly selected reflections.
‡As defined by PROCHECK.

167 ordered solvent molecules. In the crystal lattice, the molecules are densely packed, resulting in a low solvent content of 39%.

$Tim21_{IMS}$ belongs to the class of α/β mixed proteins (Fig 2A,B). In total, the secondary structure is composed of two α-helices (α1 and α2) and eight β-strands (β1–β8) connected by loops, some of which are extended but nonetheless well defined. About 50% of the residues are part of well-defined secondary structure elements (Fig 2B,C). At the N terminus, the chain folds into a four-repeat long α-helix followed by a short loop that connects α1 helix to the tilted α2 helix. The α1 helix is flanked by the antiparallel β-strands

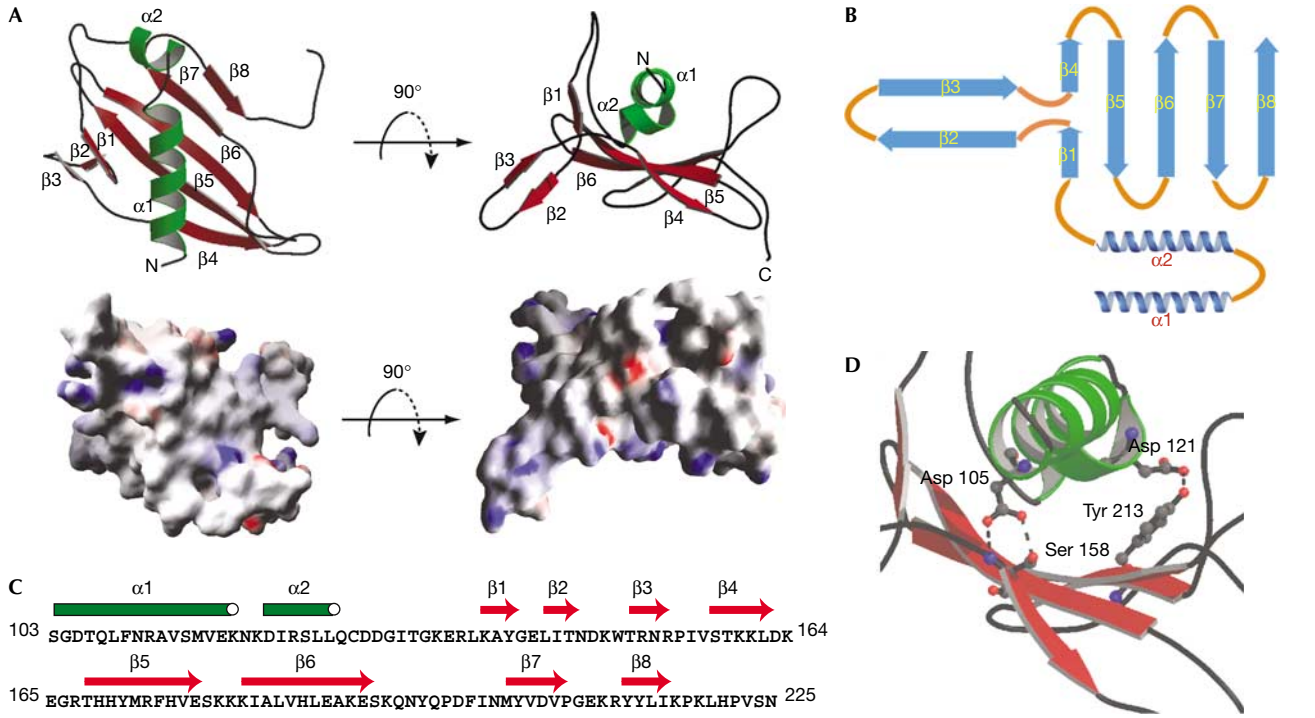

Fig 2 | Crystal structure of $Tim21_{IMS}$. (**A**) Views of the molecular structure of $Tim21_{IMS}$ (top) with labelled α-helices (green) and β-strands (red). Images were generated using Molscript (Kraulis, 1991). Surface presentations of the $Tim21_{IMS}$ molecule are shown (bottom). Positive and negative potentials are coloured blue and red, respectively. The images were generated using Grasp (Nicholls *et al*, 1991). (**B**) Schematic representation of the $Tim21_{IMS}$ fold. (**C**) Sequence of $Tim21_{IMS}$ and distribution of secondary structure elements. (**D**) Hydrogen bonds (dashed) between the helical part and the antiparallel β-sheet. $Tim21_{IMS}$, translocase of the inner membrane.

β4–β8, which together form an extended β-sheet. Three hydrogen bonds exist between the helices and the β-sheet (Fig 2D; supplementary Table 1 online). Helix α1 is flanked by two loop structures—the extended loop connects β-strands 6 and 7 to the right side, and parts of the loop connect the α2 helix and β1 to the left side. Residues 219–225 are stabilized in the crystal lattice by interactions with neighbouring molecules of the crystal packing. A DALI database search for structures related to $Tim21_{IMS}$ did not find a protein with a similar fold; thus, we conclude that the $Tim21_{IMS}$ structure represents a new protein fold.

Negative charges in Tom22–Tim21 interaction

Surface-exposed residues of $Tim21_{IMS}$, which were conserved between different species, were grouped into four classes—positively charged, negatively charged, amphipathic residues, and hydrophobic residues. Patches of positively charged residues represented the most abundant form of the exposed conserved residues (Fig 3). By contrast, $Tom22_{IMS}$, consisting of the C-terminal 33 residues, has a net charge of −5 (Court *et al*, 1996; Moczko *et al*, 1997; Komiya *et al*, 1998). The different charge distribution between $Tim21_{IMS}$ (with a net charge of +8) and $Tom22_{IMS}$, and the reported inhibition of the Tim21–Tom22 interaction by positively charged presequences (Chacinska *et al*, 2005), raised the possibility that electrostatic interactions are involved in the binding of Tim21 to the TOM complex.

To analyse the interaction between the IMS domain of Tim21 and the TOM complex, the purified domain was attached to an affinity column and incubated with solubilized mitochondria (Chacinska *et al*, 2005). Although the TOM complex efficiently bound to Tim21 at 80 mM NaCl, the interaction was strongly decreased on washing with higher salt concentrations (Fig 4A). This salt sensitivity indicates an involvement of electrostatic interactions in the binding of Tim21 to the TOM complex.

We examined which regions of Tom22 are required for interaction with Tim21. A Tom22 peptide library, comprising the region from the membrane span to the C terminus, was probed with the purified IMS domain of Tim21, followed by quantitative analysis. Binding was maximal in a region between residues 123 and 147 (supplementary Fig 1A online). We then analysed three peptides for an interaction with $Tim21_{IMS}$ in solution: the entire 33-residue $Tom22_{IMS}$ (P1); a 23-residue fragment (P2); and a 17-residue fragment (P3; Fig 4B). All three peptides were crosslinked to $Tim21_{IMS}$ (Fig 4C). The shortest peptide P3, corresponding to residues 131–147—that is, the peak and plateau area of binding to the peptide library—was linked to $Tim21_{IMS}$ with an efficiency similar to that with full-length $Tom22_{IMS}$. We thus studied whether this short peptide affected the interaction of $Tim21_{IMS}$ with Tom22 in the context of the *in vivo/in organello* situation, that is, when full-length Tom22 was present in the TOM complex and the complete set of mitochondrial proteins was present. The peptide indeed impaired the interaction of $Tim21_{IMS}$ with the TOM complex in solubilized mitochondria (supplementary Fig 1B online). Taken together, we conclude that the segment of Tom22 represented by P3 contains sufficient information for binding to Tim21.

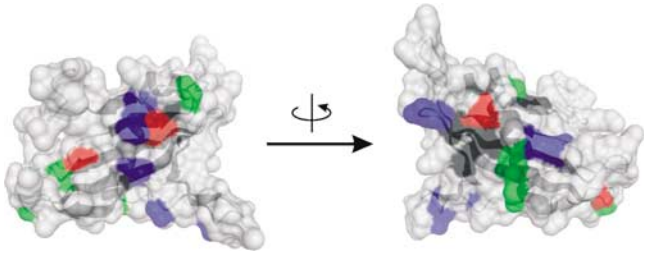

Fig 3 | Surface presentations of $Tim21_{IMS}$. Conserved positively charged (blue), negatively charged (red), amphipathic (green) and hydrophobic (black) residues on the surface are shown. Ten unicellular organisms were compared (*Saccharomyces cerevisiae*, *Aspergillus fumigatus*, *Neurospora crassa*, *Candida albicans*, *Kluyveromyces lactis*, *Aphis gossypii*, *Candida glabrata*, *Desulfomusa hansenii*, *Yarrowia lipolytica*, *Schizosaccharomyces pombe*). Images were generated using DINO (http://www.dino3d.org/). $Tim21_{IMS}$, translocase of the inner membrane.

We systematically replaced the five charged residues of P3 by alanines and analysed the interaction of the modified peptides with $Tim21_{IMS}$ by crosslinking (Fig 4C, lanes 7–13). A replacement of both Asp 131 and Asp 135 blocked the interaction of P3 with $Tim21_{IMS}$, whereas the interaction took place when the two other negatively charged residues (Glu 144 and Asp 146) or the positively charged Lys 145 were replaced. We studied whether the replacement of Asp 131 and Asp 135 affected the influence of P3 on the interaction of $Tim21_{IMS}$ with the TOM complex under *in organello* conditions. Indeed, the modified peptide P3-D131A,D135A did not compete for binding of full-length Tom22 to $Tim21_{IMS}$, in contrast with the wild-type form of P3 (supplementary Fig 1C online). The crucial role of two aspartate residues thus supports the model of an electrostatic interaction between Tom22 and Tim21.

CONCLUSIONS

We solved the structure of the binding domain of Tim21 that contains a new mixed α/β-protein fold. The surface of Tim21 shows patches of conserved, positively charged residues and interacts with the negatively charged IMS domain of Tom22. Binding of Tim21 to Tom22 involves electrostatic interactions, with a 17-residue segment of $Tom22_{IMS}$ being sufficient for binding to $Tim21_{IMS}$. Two negatively charged residues in this core segment of $Tom22_{IMS}$ are involved in the association with $Tim21_{IMS}$. An electrostatic interaction between Tim21 and Tom22 agrees with the observation that the positively charged presequences compete with Tim21 for binding to Tom22 (Chacinska *et al*, 2005). Tim21 represents the first structure of a component of the mitochondrial presequence translocase, as well as of a component that connects protein complexes located in the outer and inner membranes of the mitochondria.

METHODS

Protein interaction analysis. $Tim21_{IMS}$ (190 μM) was incubated with a twofold molar excess of Tom22 peptides in 10 mM HEPES, 50 mM NaCl, 50 mM KCl and 3 mM $MgCl_2$. Glutaraldehyde was added at 0.02% and the mixture was incubated at 30 °C for 15 min, followed by SDS–polyacrylamide gel electrophoresis. Salt-dependent interaction of the IMS domain of Tim21 with the TOM complex was analysed as described previously (Chacinska *et al*, 2005), except that the wash buffer contained

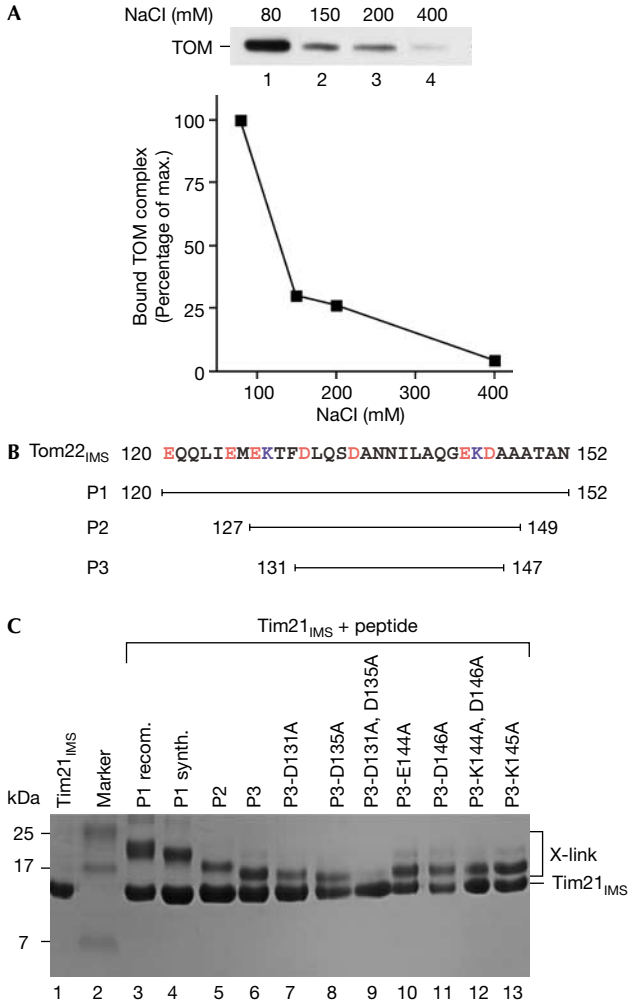

Fig 4 | The $Tim21_{IMS}$–$Tom22_{IMS}$ association involves electrostatic interaction. (**A**) The immobilized IMS domain of Tim21 was incubated with solubilized yeast mitochondria. After washing in the presence of NaCl, bound proteins were eluted and analysed by SDS–polyacrylamide gel electrophoresis (SDS–PAGE) and western blotting with Tom40 antibodies. (**B**) Sequence of $Tom22_{IMS}$ and synthetic peptides. (**C**) Isolated $Tim21_{IMS}$ was incubated with purified $Tom22_{IMS}$ (P1 recom.) or the indicated peptides and crosslinked with glutaraldehyde. Samples were analysed by SDS–PAGE and Coomassie staining. $Tim21_{IMS}$, translocase of the inner membrane; $Tom22_{IMS}$, translocase of the outer membrane.

the indicated amounts of NaCl. ^1H NMR spectra were recorded on a DRX-500 spectrometer (Bruker BioSpin, Billerica, MA, USA) at 27 °C. $Tim21_{IMS}$ (5.3 mM in 10 mM HEPES and 50 mM NaCl (pH 7.5)) was added stepwise to $Tom22_{IMS}$ (~2.1 mM in PBS, pH 6.9; H_2O:D_2O = 9:1). Water suppression was achieved using the WATERGATE sequence (Sklenar *et al*, 1993) and data processing was carried out using XWINNMR-v3 (Bruker). Protein expression and purification are described in the supplementary information online.

Protein crystallization and data collection. Crystallization was carried out by the hanging-drop set-up by mixing 1 μl of protein solution and reservoir solution using the Crystal Screens I and II and the Index Screen (Hampton, Aliso Viejo, CA, USA). Initial

$Tim21_{IMS}$ crystals were obtained from numbers 9 and 40 of the Crystal Screen I and from numbers 67 and 75 of the Index Screen after 2–4 weeks. Crystallization could be reproduced and improved by seeding. SeMet protein crystals were obtained from variations of number 75 of the Index Screen by seeding with crystals of the native protein. Best results were achieved with 20% (w/v) polyethylene glycol 3350, 0.2 M Li_2SO_4 and 0.1 M Bis–Tris (pH 6.5). Before measurement, crystals were stabilized in crystallization buffer supplemented with 15% (v/v) glycerol or 20% (w/v) xylitol and flash frozen in liquid nitrogen. A native data set with a resolution limit of 1.6 Å was obtained at beamline BW6 (DESY, Hamburg, Germany). For structure solution, a MAD experiment was carried out on an SeMet crystal at beamline ID29 (ESRF, Grenoble, France). Data were recorded at Se peak, inflection and remote energies to a resolution limit of 1.9 Å (Table 1).

Structure determination, model building and structure refinement. Images were indexed, integrated and scaled using the XDS program package (Kabsch, 1993). Three of the four Se atoms could be located with the Patterson routine implemented in the program SOLVE, and density modification was carried out in RESOLVE (Terwilliger, 2000). A partial model consisting of amino acids 104–161 and 171–216 was automatically generated with the program ARP/wARP (Lamzin *et al*, 2001). Inspection of the model, refinements, improvements of density maps and manual completion of the molecule were carried out using repetitive combinatorial cycles of the programs 'O' (Jones *et al*, 1991) and CNS (Brunger *et al*, 1998). Water molecules were picked automatically using CNS and their positions included in the refinements. During the refinement rounds, 5% of the reflections were used for cross-validation. The cloning and TEV cleavage-derived additional amino acids could not be seen in the electron density map. The stereochemical quality of the model was validated with PROCHECK (Laskowski *et al*, 1993). The coordinates and diffraction amplitudes were deposited in the RCSB Protein Data Bank with accession code 2CIU.

Supplementary information is available at *EMBO reports* online (http://www.emboreports.org).

ACKNOWLEDGEMENTS

We thank S. Uebel and co-workers, and the staffs of beamlines BW6 (Deutsches Elektronen-Synchrotron) and ID29 (European Synchrotron Radiation Facility) for their support and R. Wagner and J. Schneider-Mergener for discussion. We are grateful to I. Perschil, A. Schulze-Specking and E. Weyher-Stingl for excellent technical assistance. This work was supported by the Deutsche Forschungsgemeinschaft, the Sonderforschungsbereich 388, Gottfried Wilhelm Leibniz Program, Max Planck Research Award, Alexander von Humboldt Foundation, Bundesministerium für Bildung und Forschung, and the Fonds der Chemischen Industrie.

REFERENCES

Abe Y, Shodai T, Muto T, Mihara K, Torii H, Nisnikawa S-I, Endo T, Kohda D (2000) Structural basis of presequence recognition by the mitochondrial protein import receptor Tom20. *Cell* **100:** 551–560

Brunger AT *et al* (1998) Crystallography & NMR system: a new software suite for macromolecular structure determination. *Acta Crystallogr D* **54:** 905–921

Chacinska A, Rehling P, Guiard B, Frazier AE, Schulze-Specking A, Pfanner N, Voos W, Meisinger C (2003) Mitochondrial translocation contact sites: separation of dynamic and stabilizing elements in formation of a TOM–TIM–preprotein supercomplex. *EMBO J* **22:** 5370–5381

Chacinska A *et al* (2005) Mitochondrial presequence translocase: switching between TOM tethering and motor recruitment involves Tim21 and Tim17. *Cell* **120:** 817–829

Court DA, Nargang FE, Steiner H, Hodges RS, Neupert W, Lill R (1996) Role of the intermembrane-space domain of the preprotein receptor Tom22 in protein import into mitochondria. *Mol Cell Biol* **16:** 4035–4042

Dekker PJT, Martin F, Maarse AC, Bömer U, Müller H, Guiard B, Meijer M, Rassow J, Pfanner N (1997) The Tim core complex defines the number of mitochondrial translocation contact sites and can hold arrested preproteins in the absence of matrix Hsp70–Tim44. *EMBO J* **16:** 5408–5419

Jensen RE, Johnson AE (2001) Opening the door to mitochondrial protein import. *Nat Struct Biol* **8:** 1008–1010

Jones TA, Zou JY, Cowan SW, Kjeldgaard M (1991) Improved methods for building protein models in electron density maps and the location of errors in these models. *Acta Crystallogr A* **47:** 110–119

Josyula R, Jin Z, Fu Z, Sha B (2006) Crystal structure of yeast mitochondrial peripheral membrane protein Tim44p C-terminal domain. *J Mol Biol* **359:** 798–804

Kabsch WJ (1993) Automatic processing of rotation diffraction data from crystals of initially unknown symmetry and cell constants. *Appl Crystallogr* **26:** 795–800

Koehler CM (2004) New developments in mitochondrial assembly. *Annu Rev Cell Dev Biol* **20:** 309–335

Komiya T, Rospert S, Koehler M, Looser R, Schatz G, Mihara K (1998) Interaction of mitochondrial targeting signals with acidic receptor domains along the protein import pathway: evidence for the 'acid chain' hypothesis. *EMBO J* **17:** 3886–3898

Kraulis PJ (1991) MOLSCRIPT: a program to produce both detailed and schematic plots of protein structures. *J Appl Crystallogr* **24:** 946–950

Lamzin VS, Perrakis A, Wilson KS (2001) The ARP/WARP suite for automated construction and refinement of protein models. In Rossmann MG, Arnold E (eds) *International Tables for Crystallography. Vol. F: Crystallography of Biological Macromolecules*, pp 720–772. Dordrecht, The Netherlands: Kluwer Academic

Laskowski RA, MacArthur MW, Moss DS, Thornton JM (1993) PROCHECK: a program to check the stereochemical quality of protein structures. *J Appl Crystallogr* **26:** 283–291

Moczko M, Bömer U, Kübrich M, Zufall N, Hönlinger A, Pfanner N (1997) The intermembrane space domain of mitochondrial Tom22 functions as a *trans* binding site for preproteins with N-terminal targeting sequences. *Mol Cell Biol* **17:** 6574–6584

Mokranjac D, Popov-Celeketic D, Hell K, Neupert W (2005) Role of Tim21 in mitochondrial translocation contact sites. *J Biol Chem* **280:** 23437–23440

Neupert W (1997) Protein import into mitochondria. *Annu Rev Biochem* **66:** 863–917

Nicholls A, Sharp KA, Honig B (1991) Protein folding and association: insights from the interfacial and thermodynamic properties of hydrocarbons. *Proteins Struct Funct Genet* **11:** 281–296

Perry AJ, Hulett JM, Likic VA, Lithgow T, Gooley PR (2006) Convergent evolution of receptors for protein import into mitochondria. *Curr Biol* **16:** 221–229

Rassow J, Guiard B, Wienhues U, Herzog V, Hartl FU, Neupert W (1989) Translocation arrest by reversible folding of a precursor protein imported into mitochondria: a means to quantitate translocation contact sites. *J Cell Biol* **109:** 1421–1428

Rehling P, Brandner K, Pfanner N (2004) Mitochondrial import and the twin-pore translocase. *Nat Rev Mol Cell Biol* **5:** 519–530

Schleyer M, Neupert W (1985) Transport of proteins into mitochondria: translocational intermediates spanning contact sites between outer and inner membranes. *Cell* **43:** 339–350

Sklenar V, Piotto M, Leppik R, Saudek V (1993) Gradient-tailored water suppression for $^{1}H–^{15}N$ HSQC experiments optimized to retain full sensitivity. *J Magn Reson* **102:** 241–245

Taylor AB, Smith BS, Kitada S, Kojima K, Miyaura H, Otwinowski Z, Ito A, Deisenhofer J (2001) Crystal structures of mitochondrial processing peptidase reveal the mode for specific cleavage of import signal sequences. *Structure* **9:** 615–625

Terwilliger TC (2000) Maximum-likelihood density modification. *Acta Crystallogr D* **56:** 965–972

Webb CT, Gorman MA, Lazarou M, Ryan MT, Gulbis JM (2006) Crystal structure of the mitochondrial chaperone TIM9-10 reveals a six-bladed α-propeller. *Mol Cell* **21:** 123–133

Wu Y, Sha B (2006) Crystal structure of yeast mitochondrial outer membrane translocon member Tom70p. *Nat Struct Mol Biol* **13:** 589–593